A Rocky Mountain Storm. Part II: The Forest Blowdown over the West Slope of the Northern Colorado Mountains—Observations, Analysis, and Modeling

MICHAEL P. MEYERS

NOAA/National Weather Service, Grand Junction, Colorado

JOHN S. SNOOK

Colorado Research Associates, Boulder, Colorado

DOUGLAS A. WESLEY

Cooperative Program for Operational Meteorology, Education and Training, University Corporation for Atmospheric Research, Boulder, Colorado

GREGORY S. POULOS

Colorado Research Associates, Boulder, Colorado

(Manuscript received 18 June 2002, in final form 3 January 2003)

ABSTRACT

A devastating winter storm affected the Rocky Mountain states over the 3-day period of 24–26 October 1997. Blizzard conditions persisted over the foothills and adjoining plains from Wyoming to southern New Mexico, with maximum total snowfall amounts near 1.5 m. (Part I of this two-part paper describes the observations and modeling of this blizzard event.) During the morning of 25 October 1997, wind gusts in excess of 50 m s^{-1} were estimated west of the Continental Divide near Steamboat Springs in northern Colorado. These winds flattened approximately 5300 ha (13 000 acres) of old-growth forest in the Routt National Forest and Mount Zirkel Wilderness. Observations, analysis, and numerical modeling were used to examine the kinematics of this extreme event. A high-resolution, local-area model (the Regional Atmospheric Modeling System) was used to investigate the ability of a local model to capture the timing and strength of the windstorm and the aforementioned blizzard. Results indicated that a synergistic combination of strong cross-barrier easterly flow; very cold lower-tropospheric air over Colorado, which modified the stability profile; and the presence of a critical layer led to devastating downslope winds. The high-resolution simulations demonstrated the potential for accurately capturing mesoscale spatial and temporal features of a downslope windstorm more than 1 day in advance. These simulations were quasi forecast in nature, because a combination of two 48-h Eta Model forecasts were used to specify the lateral boundary conditions. Increased predictive detail of the windstorm was also found by decreasing the horizontal grid spacing from 5 to 1.67 km in the local-area model simulations.

1. Introduction

A destructive wind event during the morning hours of 25 October 1997 affected a broad area on the western slope of the Continental Divide in northern Colorado. Wind gusts in excess of 50 m s^{-1} were observed just west of the Continental Divide. These winds were strong enough to flatten ~5300 ha (13 000 acres) of old-growth forest in the Routt National Forest and the Mount Zirkel Wilderness northeast of the town of Steamboat Springs (SBS; Fig. 1). The effective barrier height in the vicinity of the Mount Zirkel Wilderness is about 1000 m, which is roughly one-half that of the Colorado Front Range. The lower barrier height allows forest growth, which is nonexistent over the higher terrain of the Front Range. According to the U.S. Forest Service (USFS), this was the largest known forest blowdown ever recorded in the Rocky Mountain region, with an areal extent of several miles wide and 20 mi long. In addition, several hunters who were trapped by the fallen trees required nearly 2 days to exit the devastated forest, because trees were stacked up to 10 m in some locations. Very cold mountaintop temperatures around −20°C created extreme wind chill temperatures colder than −50°C.

The wind event of 25 October 1997 was unlike the more typical Colorado Front Range downslope windstorm, in that the strong winds were easterly and, there-

Corresponding author address: Michael P. Meyers, National Weather Service, 792 Eagle Dr., Grand Junction, CO 81506.
E-mail: mike.meyers@noaa.gov

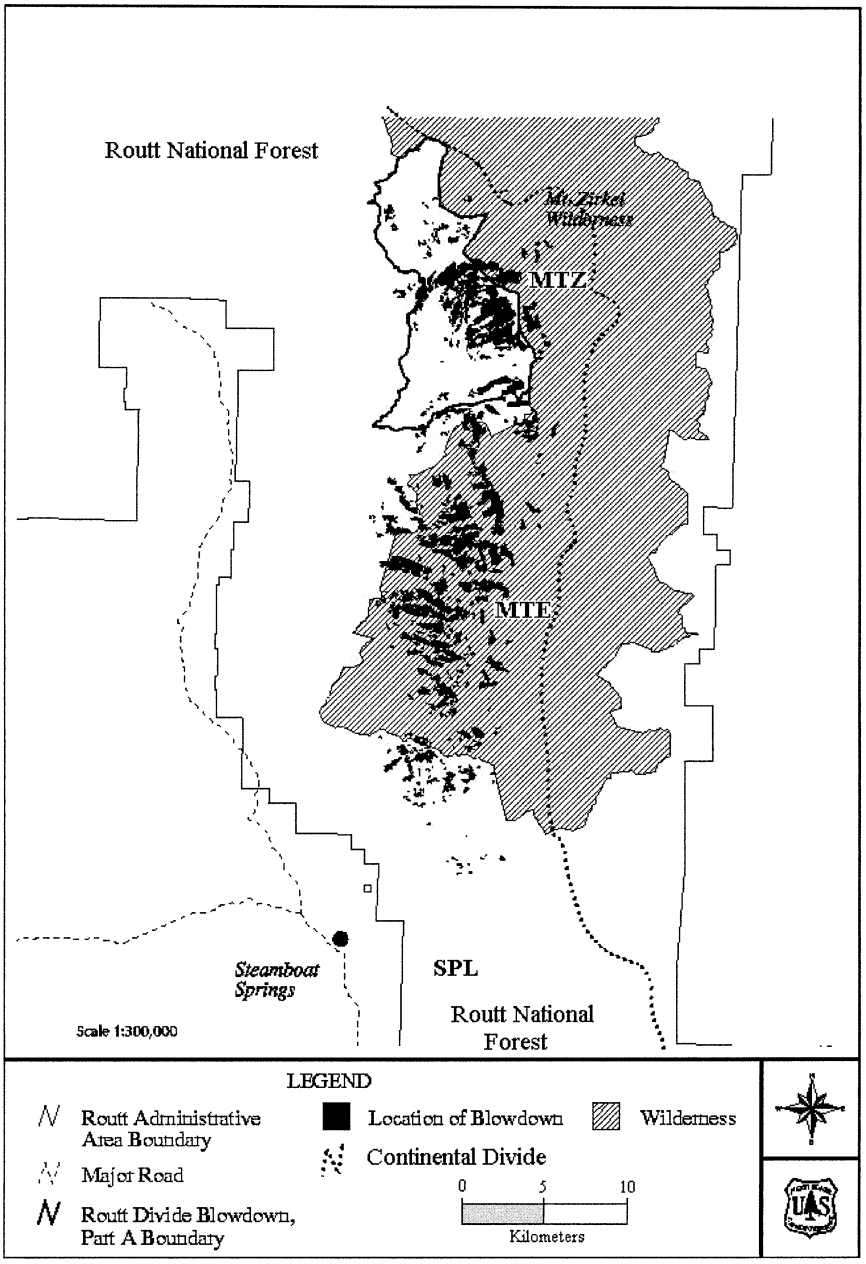

FIG. 1. Routt National Forest and Mount Zirkel Wilderness forest blowdown area. Hatched area is location of wilderness. Black shading is area of blowdown. Continental Divide is indicated by the darker dotted line. Symbols: Storm Peak Laboratory (SPL), Mount Zirkel (MTZ), and Mount Ethel (MTE). Adapted from the USFS.

fore, the damage was located to the west of the mountain barrier. This event was a result of the same winter storm that paralyzed much of the Colorado Front Range and southern Wyoming with heavy snow during the 3-day period of 24–26 October 1997. Observations showed total snowfall amounts of more than 1.0 m in many Colorado foothill and mountain locations *east* of the Continental Divide. An observational and modeling account of the snowstorm portion of this unique case is detailed in a companion article by Poulos et al. (2002, hereinafter Part I). In combination, these two impacts from a single event are unprecedented in the recorded history of Colorado weather.

Recent advances in computer technology have created the capability to generate high-resolution, local-domain numerical weather prediction (NWP) in real time using affordable computer hardware (Mass and Kuo 1998). Several projects (e.g., Cotton et al. 1994; Snook and Pielke 1995; Snook et al. 1995, 1998; Manobianco et al. 1996; Horel et al. 2002) have demonstrated the utility

of NWP in the local forecast office. Results from these studies indicate that local NWP can add value to numerical forecast guidance generated at a central facility. Local NWP is not designed to replace central-facility products, but rather it has been shown that both central-facility and local-office NWP can be used synergistically to provide a complete numerical guidance package. Indeed, the National Centers for Environmental Prediction (NCEP) suite of numerical prediction models provided good regional-scale guidance for the general area and timing of heavy snow for this event (Part I). These national-domain models, however, are not configured to provide detailed forecasts of mesoscale phenomena such as the snowfall variability and the local areas of extreme winds observed in the October 1997 Rocky Mountain storm. Local-area NWP products are designed to provide additional mesoscale prediction guidance and understanding of local weather events to the local forecast office, and their utilization here helps to define the unique mechanisms that caused the forest blowdown event.

The purpose of this study is to investigate and determine the kinematics responsible for this rare event and to assess qualitatively any additional value provided by quasi-operational local-area NWP. Consideration of these factors contributes to an understanding of what conditions forced the forest blowdown associated with the strong winds observed in this study. Numerous studies investigating downslope windstorms along the Front Range have been conducted (e.g., Klemp and Lilly 1975; Clark and Peltier 1977; Peltier and Clark 1979; Clark and Farley 1984; Durran and Klemp 1987; Lee et al. 1989; Brown et al. 1992; Cotton et al. 1995, Doyle et al. 2000), in part because of the higher frequency of high-wind events east of the Continental Divide, because the predominant winds aloft have a westerly component. None of the studies have described high-wind events resulting from easterly winds traversing the Continental Divide in Colorado. However, examples of downslope wind events caused by easterly winds in other regions, such as the Santa Ana (Svejkovsky 1985) and Croatian bora (Smith 1987), have been observed. Both Durran (1990) and Colle and Mass (1998b) describe several common characteristics found in these and other studies on downslope windstorms:

1) strong cross-barrier flow at crest level with weak vertical shear above it, where the upper-tropospheric winds are not excessively strong;
2) an inversion or layer of strong stability near the mountain crest with lower stability above;
3) the presence of a critical layer (layer of zero wind or flow reversal), which reflects gravity-wave energy downward; and
4) synoptic-scale downward forcing.

Durran (1990) further suggests that these conditions promote the development of larger-amplitude mountain waves that create an environment in which breaking waves (Clark and Peltier 1977) are more likely.

To investigate this case, an observational description of the event is documented in the next section, outlining the environmental conditions responsible for the downslope windstorm. The Regional Atmospheric Modeling System (RAMS) mesoscale model (Pielke et al. 1992) developed at Colorado State University is also used to simulate this case study. Two 60-h quasi-forecast simulations are run: the first with the use of a fine grid of 5-km grid spacing and the second with two additional fine grids of 1.67-km grid spacing. The second simulation was the same run used to examine the blizzard event over the Front Range of Colorado and Wyoming as detailed in Part I. The numerical portion of this investigation examines the longer-temporal-range forecast capabilities of local NWP and verification improvement from increased horizontal resolution.

2. Case study

The Rocky Mountain blizzard and blowdown events were characterized by strong forcing on the synoptic scale. During the day on 24 October 1997, a deep closed low developed over the Four Corners region in response to a diving jet maximum over the desert Southwest (Fig. 2a). As the surface low pressure developed over southern Colorado, strong northeast winds developed over northern Colorado and southern Wyoming as evidenced by the 850-hPa analysis at 0000 UTC 25 October (Fig. 2b), resulting in heavy snow and wind across this region. A strong northwest–southeast pressure gradient persisted through the morning hours of 25 October. West of the Continental Divide, the weather during the day of 24 October was characterized by widespread light to moderate snow, which was primarily due to large-scale forcing (Part I). After 0000 UTC 25 October, surface winds across mountain locations of northern Colorado increased dramatically, with a strong easterly component. By 1200 UTC 25 October (Fig. 3a), the 500-hPa closed low deepened slightly as it moved into northeastern New Mexico with easterly winds (40 m s^{-1}) over eastern Colorado. The 850-hPa analysis shows that the closed low had moved over the Texas Panhandle, with winds (35 m s^{-1}) having become more northerly across eastern Colorado (Fig. 3b). Figures 2b and 3b also depict the 700-hPa temperatures for 0000 and 1200 UTC 25 October, respectively. This modified arctic air mass was drawn south into the low overnight on 25 October, with the -10°C isotherm moving into northern New Mexico by 1200 UTC. The 700-hPa temperatures dropped 5°C across northern Colorado during this 12-h period.

Because of the sparsity of observations along and west of the Continental Divide, there is not much documentation of the winds. Two locations, however, did take atmospheric measurements during this event. The Arapahoe Basin Ski Area (ABS; Table 1), just west of

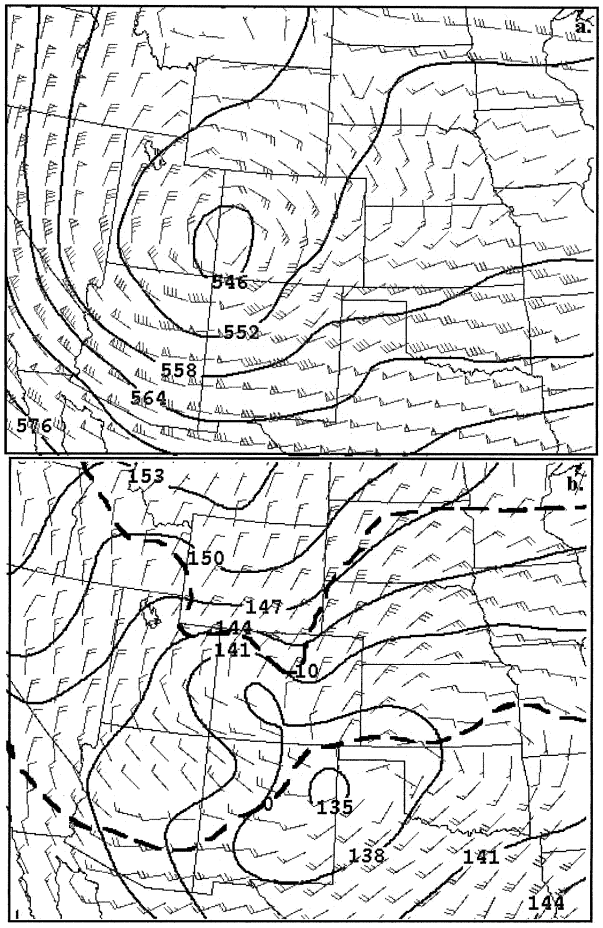

FIG. 2. (a) Rapid Update Cycle (RUC) 500-hPa analysis of heights and winds at 0000 UTC 25 Oct 1997. Heights are contoured every 6 dam. Wind barbs are in meters per second. (b) RUC analysis of 850-hPa heights and winds at 0000 UTC 25 Oct. Heights are contoured every 3 dam. Wind barbs are in meters per second. RUC analysis of 700-hPa temperatures (°C) at 0000 UTC 25 Oct is also shown. Contour interval is 10°C as indicated by the dashed line.

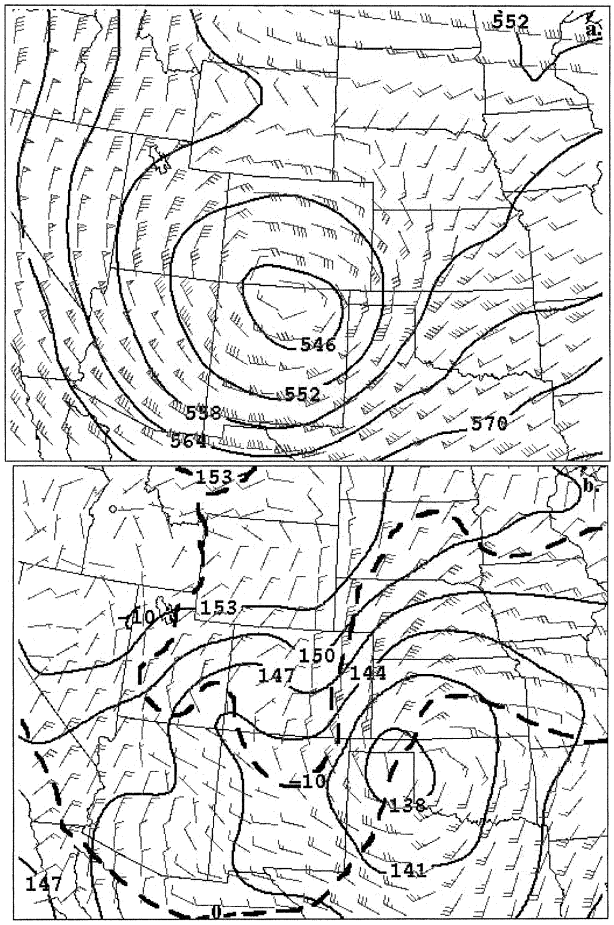

FIG. 3. Same as Fig. 2 but at 1200 UTC 25 Oct 1997.

the Continental Divide at 3800 m, measured wind gusts in excess of 40 m s^{-1} (100 mi h^{-1}) each hour between 1000 and 1700 UTC (0400 and 1100 local time), and a peak wind gust of 51 m s^{-1} (114 mi h^{-1}) from the east was recorded at 1340 UTC. Temperatures during this time period were around −20°C, resulting in wind chill temperatures below −50°C. Just several hours earlier and to the north of ABS, the extreme wind gusts flattened 5300 ha (13 000 acres) of old-growth forest in the Routt National Forest and the Mount Zirkel Wilderness. South of the blowdown area at the Desert Research Institute's Storm Peak Laboratory (SPL; Borys and Wetzel 1997) on the top of Steamboat Springs Ski Area (approximately 7 km southeast of SBS; Fig. 1), peak winds were measured at 25 m s^{-1} around 0800 UTC 25 October. However, no evidence of forest blowdown occurred in the vicinity of SPL, with all of the forest blowdown occurring north of SPL as indicated in Fig. 1.

TABLE 1. Area observations at Arapahoe Basin Ski Area (elev 3800 m) on 25 Oct 1997.

Hour (UTC)	Min temperature (°C)	Peak wind gust (m s^{-1})	Wind speed (m s^{-1})	Direction (°)
0600	−19	26	13	18
0700	−19	33	10	21
0800	−19	37	14	23
0900	−20	33	17	37
1000	−20	44	19	46
1100	−20	40	21	43
1200	−21	49	32	39
1300	−20	49	32	86
1400	−19	51	30	71
1500	−19	47	31	78
1600	−18	48	29	83
1700	−18	44	22	101
1800	−17	37	21	118
2000	−16	38	19	123
2100	−16	29	13	137
2200	−15	23	9	156
2300	−14	28	12	140

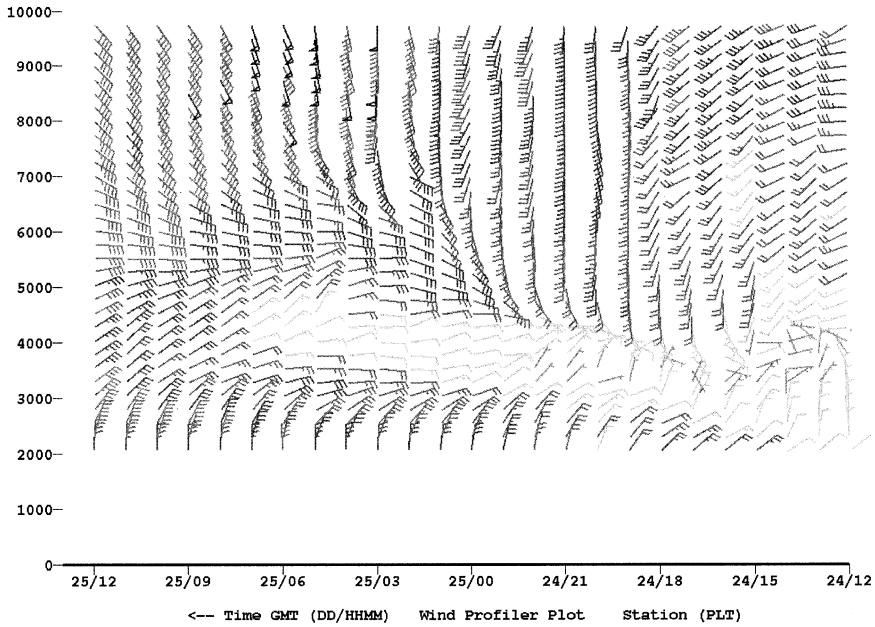

FIG. 4. The Platteville, CO, wind profile (kt) from 1200 UTC 25 Oct 1997 to 1200 UTC 24 Oct 1997. Platteville is located approximately 50 km north of Denver, CO. Ordinate is height (MSL) in meters.

Observational data indicated that the potential of strong winds occurring over the Colorado mountains existed during the morning of 25 October. Wind profiler data at Platteville, Colorado (PTL; Fig. 4), located approximately 50 km north of Denver, depict the evolution of the wind profile with time on 24 and 25 October. As the cutoff low pressure system (Fig. 2b) developed over the Texas Panhandle by 0000 UTC 25 October, the layer of predominantly easterly winds [~3000 m above mean sea level (MSL)] strengthened significantly and deepened. As noted earlier, the onset of strong easterly winds was observed along and west of the Continental Divide during the morning hours of 25 October. This timing coincides with the onset of strong winds evident in the PTL profiler data.

Model guidance from NCEP also showed support for strong winds west of the Continental Divide. Figure 5 show short-range 1500 UTC 24 October Meso Eta Model forecasts of wind speed, potential temperature, and vertical motion for a vertical cross section extending from Grand Junction, Colorado, to Scottsbluff, Nebraska, valid at 0900 UTC 25 October. Figure 5a shows that the model did predict significant low-level winds (~25 m s^{-1}) to the west of the Continental Divide over northern Colorado. Upstream stability below 500 hPa (4.0°–4.5°C km^{-1}) was significant (Fig. 5b) both in the short-range Meso Eta forecast and the observed Denver sounding at 1200 UTC 25 October (not shown); however, the environment was less stable above 500 hPa.

A typical measure of the upstream blocking and the potential for nonlinear behavior is expressed by the dimensionless quantity called the Froude number:

$$\mathrm{Fr} = U/NH,$$

where U is the upstream wind speed and N is the Brunt–Väisälä frequency representative over the mountain depth H (Carruthers and Hunt 1990). There are some concerns with the use of Fr in an unbounded realistic atmosphere, despite it widespread use. That is, Fr was first defined for shallow-water theory in which the density interface is a step function (e.g., Durran 2002). Also, whereas the theory allows for constant N and U, no such simple upstream state exists in this case study. However, the fact that the upstream environment here contains a significant stability interface at ~500 hPa allows for the application of $\overline{U}$ and $\overline{N}$, which are the mean upstream wind speed and Brunt–Väisälä frequency through the mountain depth h. Approximating $\overline{U} = 15$ m s^{-1} and $\overline{N} = 0.016$ s^{-1} from model guidance, with an effective barrier height of 2000 m for the Front Range, a Froude number of ~0.5 was measured for the north-central portion of Colorado during this time. Other calculations using estimated wind and stability from the model guidance with an effective barrier height of 1000 m for the Mount Zirkel Wilderness yielded Froude numbers between 0.5 and 0.7. These values correspond to partially blocked flow, nonlinear flow behavior, including acceleration to the lee of the barrier, and possible wave breaking (e.g., Klemp and Lilly 1975; Poulos et al. 2000). Poulos et al. (2000) presented numerical modeling evidence that winds can increase on the lee side by a factor of 2.5 or more when compared with the upstream mountaintop-level wind under conditions with the Froude number near 0.5 (a variety of methods were tested, all

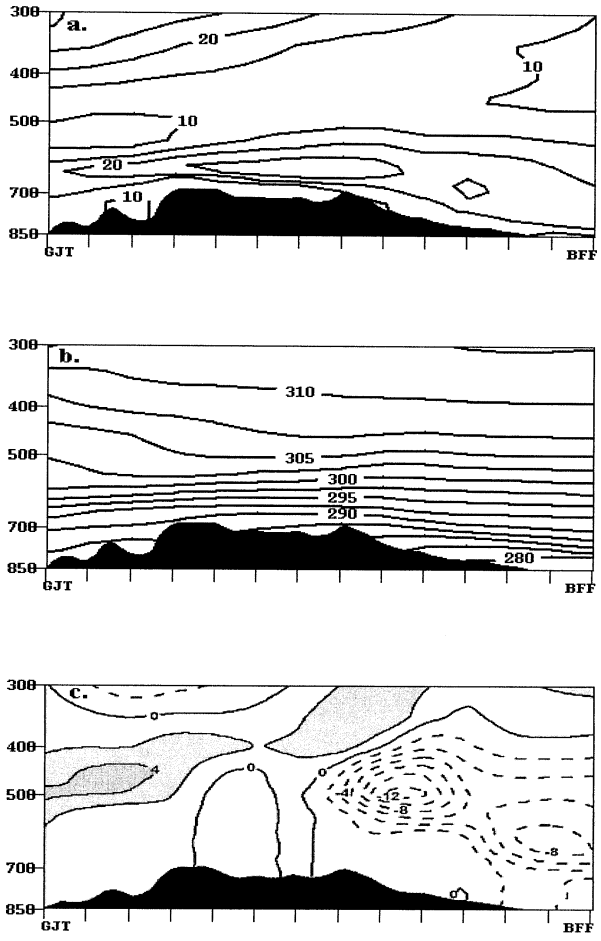

FIG. 5. Short-range Meso Eta Model forecasts of (a) wind speed (contour interval is 5 m s^{-1}), (b) potential temperature (contour interval is 2.5 K), and (c) vertical motion (contour interval is 2 μbar s^{-1}, with downward motion shaded) for a vertical cross section extending from Grand Junction, CO (GJT), to Scottsbluff, NE (BFF). Vertical coordinate is in pressure (hPa). All figures are 18-h forecasts valid at 0900 UTC 25 Oct 1997.

of which fell in the nonlinear regime). The potential temperature profile (Fig. 5b) also showed a stable lower troposphere and a decrease in stability in the middle and upper troposphere. Smith (1985) and Durran (1986) have noted that conditions similar to these can switch the atmosphere to supercritical flow over a mountain barrier (in which the flow over the barrier continues to accelerate as it descends along the leeward slope) and produce strong downslope winds at the surface. Strong ascent caused by terrain and large-scale forcing was predicted by the Meso Eta Model (Fig. 5c) over eastern Colorado, but much of the West Slope of Colorado was influenced by synoptically forced downward motion.

The observations and NCEP model guidance indicated conditions were favorable for strong winds west of the Continental Divide during the morning of 25 October. The performance of the models benefited from the fact that the 24–26 October 1997 storm was forced strongly on the large scale. However, quantitative predictions of surface winds from NCEP guidance were nearly a factor of 3 lower than observed. Recent literature has documented shortcomings of the Eta vertical coordinate system in complex topographic regions that may account for this underprediction of the winds (Gallus 2000; Gallus and Klemp 2000). Another possible explanation for the underprediction of the winds may be the fact that the Eta Model at the time had a horizontal grid spacing of 48 km. There have been several investigations that have documented verification improvement with regard to wind speed in orographic environments when the horizontal grid spacing is decreased to below 10 km (McQueen et al. 1995; Colle and Mass 1998a, 2000). Doyle and Smith (2002) noted more recently that decreasing the grid spacing from 4 to 1 km improved the capability of the model in resolving a lee wave over the Hohe Tauern. Mass et al. (2002) summarized the results of an objective multiyear verification over western Washington State. In their investigation, there was a clear improvement found as the grid spacing was decreased from 36 to 12 km, with only small improvements found as the grid spacing was decreased from 12 to 4 km. Mass et al. mention that these findings may be overly pessimistic and that the 4-km forecasts generated more detail and structure, which may not have had an impact on the traditional objective verification scores. They also point out that a sparse observational network further hinders verification as the grid spacing decreases. The nested-grid simulations described in the following sections address the issues of using alternative horizontal grid resolutions in a high-wind event over complex topography.

3. Local-model simulations

Numerical investigations performed in a ''research mode'' setting 10 years ago are now run in an operational environment today. As computer power continues to increase, the research-mode simulations of today will be the operational standard of tomorrow. The case study simulations presented in this section use higher grid resolutions with a longer forecast period to evaluate two questions: 1) does higher horizontal grid resolution produce more accurate high-wind predictions for the blowdown and 2) can the mesoscale details of these systems be predicted more than 1 day in advance?

Two simulations were conducted using a nonhydrostatic nested-grid version of RAMS. In the first simulation, a single nest was used. In the second simulation, two additional finer-scale grids were employed to examine the high winds that occurred during the forest blowdown. Next, the experiment design and forecast results for both simulations are presented.

a. Experiment design

To investigate both the forest blowdown west of the Continental Divide and the blizzard over eastern Col-

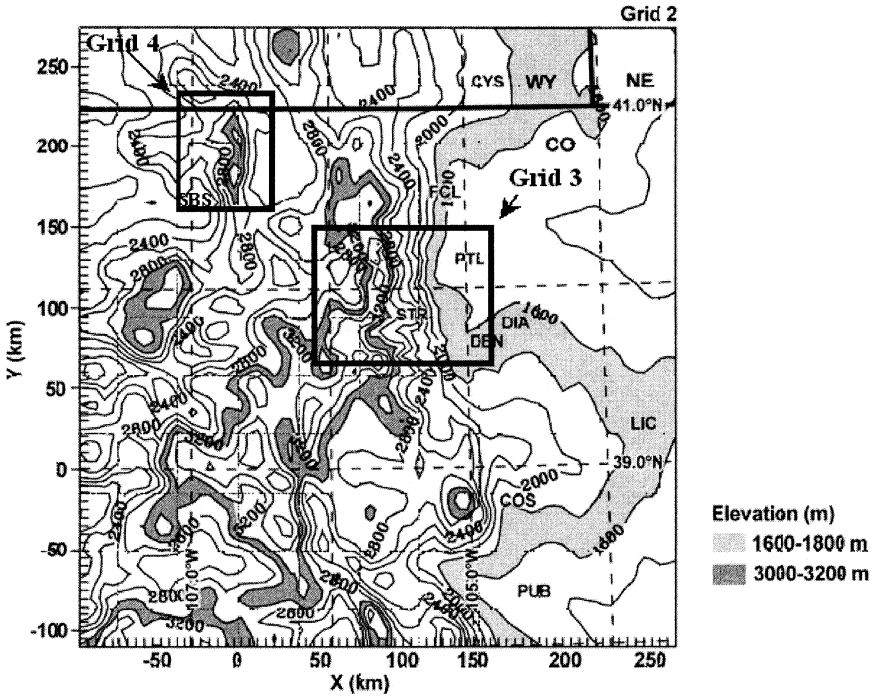

FIG. 6. The topography (200-m contour interval) from grid 2. The southwest corner is 38.01°N, 107.79°W. Latitude and longitude lines (dashed) are 1.0° intervals. Grid 3 and grid 4 ($\Delta x = \Delta y = 1.67$ km) domains are also shown. Symbols: Steamboat Springs (SBS), Denver (DEN), Denver International Airport (DIA), Cheyenne, WY (CYS), Platteville wind profiler (PTL), Limon (LIC), Colorado Springs (COS), and Pueblo (PUB).

orado, these quasi-forecast runs utilize the nonhydrostatic nested-grid version of RAMS to generate 60-h simulations. The analyses and the 6-h forecast from the 0000 UTC 24 October 1997 NCEP operational 48-km Eta Model (Black 1994) are used to initialize and provide the 6-h lateral boundary conditions for this RAMS run. Because the Eta had a forecast duration of 48 h in 1997, we used the analysis and each subsequent 6-h forecast from the 1200 UTC 24 October 1997 Eta Model as forecast lateral boundary conditions for the RAMS simulation from 12- out to 60-h simulation time (1200 UTC 26 October 1997). Because of the unique initialization and boundary conditions, the experiments would be a better representation of a true forecast from the 1200 UTC 24 October initialization.

In the preliminary simulation (simulation I), the outermost grid encompasses Colorado and a portion of the surrounding states with a 15-km grid spacing (61 × 61). Grid 2 (Fig. 6) employs a 3:1 nest ratio with a 5-km grid spacing (77 × 80). The higher-resolution run (simulation II) uses the identical design of simulation I, except for two additional nests (grid 3 and grid 4—depicted in Fig. 6) to capture the finescale detail needed for this investigation. Grids 3 (68 × 53) and 4 (32 × 41) use a 1.67-km grid spacing. Grid 3 is positioned along the Colorado Front Range to capture the heavy upslope precipitation, as documented in Part I, and the high winds at the Arapahoe Basin Ski Area. Grid 4 is located northeast of SBS to cover the forest-blowdown region. Part I examines the sensitivity of two different microphysical schemes [Walko et al. (1995) and Schultz (1995)] on the heavy-snow event. For the high-wind investigation, however, the outcome is nearly identical for both microphysical schemes, and therefore only the results using the Walko et al. physics are discussed.

b. Simulation I: Single-nest configuration

Figure 7 shows a horizontal depiction of the 34-h wind forecast from the RAMS 5-km grid at the lowest model level [~50 m above ground level (AGL)] valid at 1000 UTC 25 October. The forecast indicates a north–south extension of winds that exceed 15 m s^{-1}, with peak values of 20 m s^{-1}. This area of higher winds extends just to the west of the higher terrain along the Continental Divide and corresponds well to the area of forest destruction; however, the magnitude of the wind speeds are underforecast, based on the amount of forest destruction. The discrepancy is partially due to the model predicting a sustained wind, and it is unrealistic to expect the model to capture the strength of peak gusts using these model grid resolutions. SPL is located just west of the strongest winds near the 15 m s^{-1} contour.

A west-to-east vertical cross section through the region of strongest winds north of SBS is depicted in Fig. 8 for the 34-h RAMS forecast valid at 1000 UTC 25

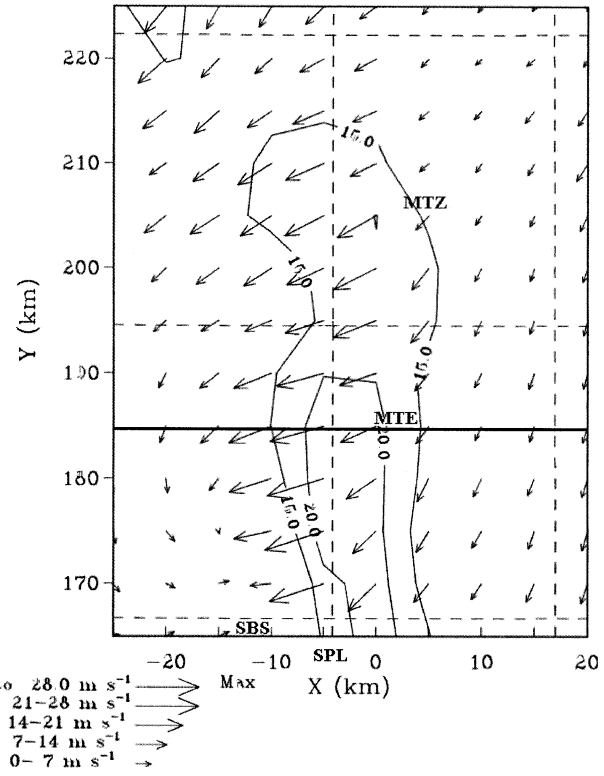

FIG. 7. Plan view of wind speed (m s^{-1}) at 50 m AGL on grid 2 for simulation I after 34 h of simulation time, valid at 1000 UTC 25 Oct 1997. Wind speed contour interval is 5 m s^{-1} (minimum contour level is 15 m s^{-1}). Wind arrows are plotted every grid point, with speed legend at bottom of figure. The figure is focused over the blowdown area. The solid horizontal line indicates the cross-sectional location shown in Fig. 8. Note that SPL is located just outside of the grid box.

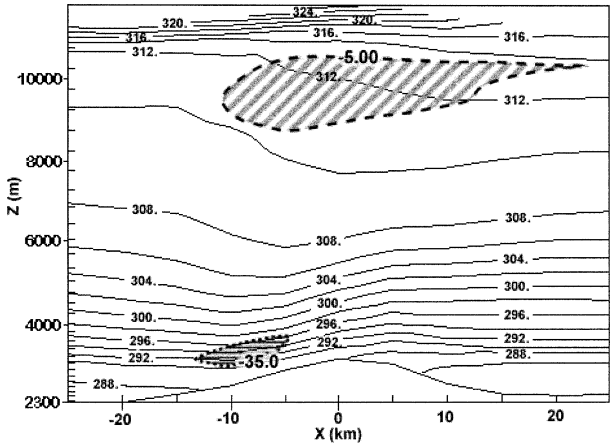

FIG. 8. West-to-east vertical cross sections on grid 2 at $Y = 185$ km (solid horizontal line in Fig. 7) after 34 h of simulation time, valid at 1000 UTC 25 Oct 1997, with potential temperature (2-K intervals) for simulation I. The U component of the wind is shaded [less than -35 m s^{-1} (near 3000 m MSL) and greater than -5 m s^{-1} (near 9500 m MSL)].

October. As noted earlier, Froude numbers were estimated to be around 0.5, which corresponds to partially blocked flow, acceleration to the lee of the barrier, and possible wave breaking. The cross section suggests that the destructive winds that occurred over the Mount Zirkel Wilderness were a result of downslope winds forced by easterly winds flowing over the Continental Divide. The simulation shows a very stable lower troposphere and a less stable middle and upper troposphere. The very stable boundary layer is partly a result of unusually cold air that advected south across the area between 0000 and 1200 UTC on 25 October. Peak easterly winds of 36 m s^{-1} are found to the lee of the Continental Divide (in proximity to the blowdown area), with a relative wind speed minimum of 3 m s^{-1} (easterly) at approximately 9500 m MSL. Even though the flow does not reverse, the cross-barrier flow approaches zero.

Figure 9 shows high winds along the Continental Divide west of Denver in the vicinity of ABS (20 m s^{-1}), but again the magnitude of the wind speeds is weaker than the observed values. Another area of high winds was forecast on the northwest portion of the grid along and west of the Continental Divide in Grand County. Although high winds and forest destruction were not observed in this sparsely populated area of Grand County, which is mostly above treeline, it is reasonable to expect that high winds did occur in this region. Model-predicted winds are comparable in magnitude to those at ABS and the forest blowdown region northeast of SBS. This result suggests that peak wind gusts in the blowdown region were on the same order of magnitude as the 50 + m s^{-1} gusts observed at Arapahoe Basin. This is consistent with the USFS (D. Pipher 1998, personal communication) estimates of 54 m s^{-1} (120 mi h^{-1}) peak winds based on visual inspection of the forest damage.

c. Simulation II: High-resolution multiple-nest configuration

Simulation II includes grid 3 and grid 4 (1.67-km grid spacing) as detailed in section 3a. Grid-4 topography is shown in Fig. 10. The 34-h RAMS forecast, valid at 1000 UTC 25 October (approximately the time of strongest observed winds over the Routt National Forest), of winds at the lowest model level (50 m AGL) for grid 4 is illustrated in Fig. 11. A north–south elongated region of easterly winds in excess of 20 m s^{-1} is similar in extent but stronger than in simulation I. SPL is located outside of the strongest wind speeds (near the 15 m s^{-1} contour). Two areas of maximum wind speeds reaching 28 m s^{-1} are embedded within the elongated region. These maxima are positioned to the lee of the two most prominent peaks in the region, Mount Zirkel (3725 m) and Mount Ethel (3640 m) (Fig. 9). Forest blowdown observations (Fig. 1; L. Drogosz, USFS, 1998, personal communication) indicated more widespread damage in the lee of these higher peaks. These

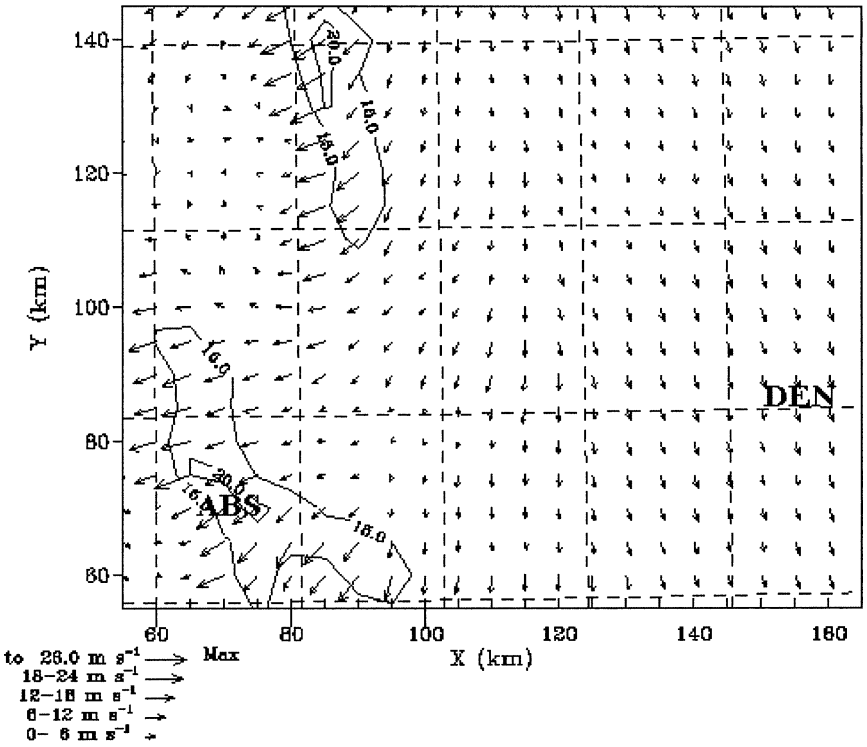

FIG. 9. Same as Fig. 7 but after 38 h of simulation time, valid at 1400 UTC 25 Oct 1997, and the figure is focused over the southern portion of grid 2.

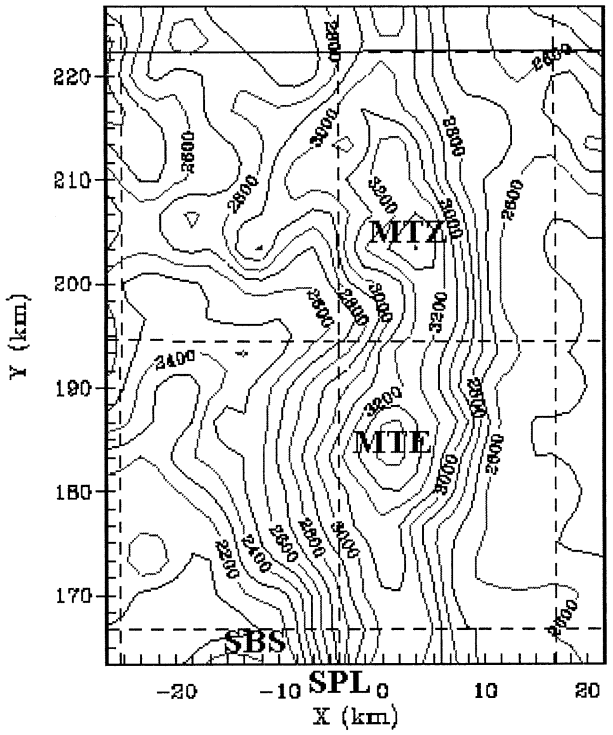

FIG. 10. Grid-4 topography (m), with contour interval of 100 m. Location of grid 4 is shown in Figure 6. Note that SPL is located just outside of the grid box.

maxima are not evident in simulation I in which a coarser grid spacing and topography are used.

A west-to-east vertical cross section through the southern wind maximum from the 34-h RAMS forecast is depicted in Fig. 12, which shows a much more pronounced mountain wave than in simulation I. Peak easterly winds of 43 m s^{-1} (20% stronger than simulation I) are found to the lee of the barrier (in proximity to the blowdown area) with a flow reversal (3 m s^{-1} westerly winds) at approximately 8000 m MSL. This flow reversal is evidence of a broad critical layer in simulation II. However, only a weakening of the cross-barrier wind to near zero is evident in simulation I.

From a forecaster's perspective, it is important to capture the timing as well as the intensity of the event. Figure 13 shows the time–height evolution of a point in grid 4 at which the strongest winds were simulated (location is immediately west of MTE in Fig. 10). The vertical component of the wind shown in Fig. 13a shows an extended period of strong downward velocity from 0000 to 0600 UTC on 25 October. From 0600 to 1030 UTC, an evolution in the vertical structure takes place in which the downward vertical velocity strengthens to nearly 5 m s^{-1} by 0800 UTC. By 1030 UTC, the flow reverses and an upward vertical velocity of 1 m s^{-1} is predicted. The horizontal component (u component) of the wind (Fig. 13b) shows a persistent pattern of very strong winds from 0000 to 0600 UTC. However, by 0600 UTC the horizontal winds increase by nearly 50%

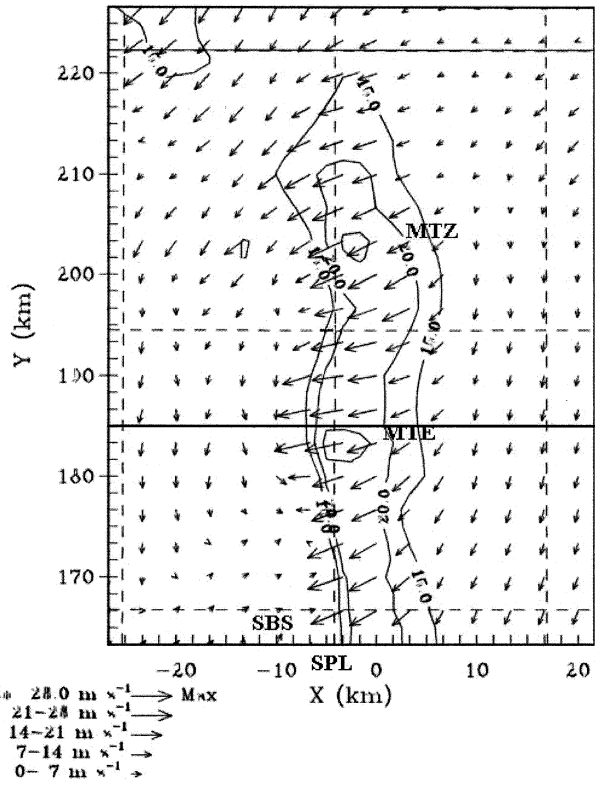

FIG. 11. Plan view of wind speed (m s^{-1}) on grid 4 after 34 h of simulation time, valid at 1000 UTC 25 Oct 1997 for simulation II. Wind speeds are contoured every 5 m s^{-1}, with minimum contour 15 m s^{-1}. Wind arrows are plotted every other grid point, with speed legend at bottom of figure. The solid horizontal line indicates the cross-sectional location shown in Fig. 12. Note that SPL is located just outside of the grid box.

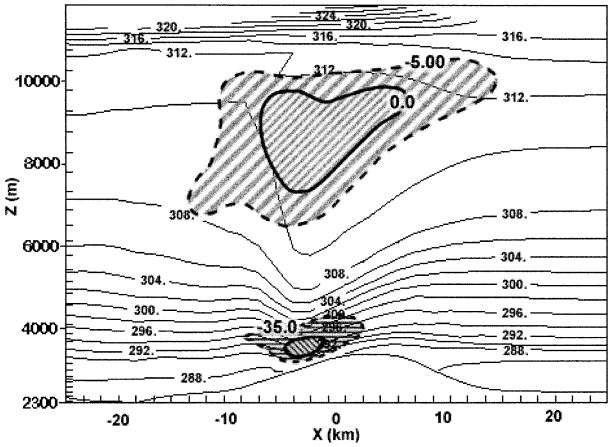

FIG. 12. West-to-east vertical cross sections on grid 4 at $Y = 185$ km (solid horizontal line in Fig. 11) after 34 h of simulation time, valid at 1000 UTC 25 Oct 1997, with potential temperature (2-K intervals) for simulation II. The U component of the wind is shaded (near 3500 m MSL: horizontal stippling denotes less than -35 m s^{-1} and vertical stippling denotes less than -40 m s^{-1}; near 8000 m MSL: thick stippling denotes greater than -5 m s^{-1} and thin stippling denotes greater than 0 m s^{-1}).

(300–800 m AGL) to a maximum of 46 m s^{-1}, which compares well with observed accounts of the strongest winds occurring between 0700 and 1000 UTC.

A plan view of the wind speeds on grid 3 is shown in Fig. 14. An area of high winds with peak speeds of 26 m s^{-1} is found near ABS. Similar to Fig. 9, another area of high winds of about 20 m s^{-1} is found along and west of the Continental Divide in Grand County, which is located in the northwestern portion of the grid. Figure 15 shows a vertical time series on grid 3 over ABS. The onset of strongest winds near the surface is forecast around 1000 UTC. Winds slowly diminish after 1800 UTC, with a further weakening of winds around 0000 UTC on 26 October. This timing compares very well with the winds shown in Table 1.

4. Discussion and conclusions

The findings from the high-resolution, local-area model forecast highlight several of the features that came together, resulting in a rare event of old-growth forest blowdown on 25 October 1997. The effective barrier height in the vicinity of the Mount Zirkel Wilderness is relatively low by Rocky Mountain standards, with an average height of about 1000 m, which is roughly one-half that of the Colorado Front Range. The lower effective barrier height allows forest growth, which is nonexistent over the higher terrain of the Front Range. The fact that old-growth forest exists in the areas northeast of Steamboat Springs is testimony to the rare nature of this event. The indication of very strong downslope winds over a relatively low barrier demonstrates the importance of nonlinear effects in this event. Forecast model output corroborates this argument as evidenced by a favorable upstream Froude number (nonlinear flow regime), the generation of a wave-induced critical layer, and enhanced cross-barrier wind speeds beneath this layer.

Observations and forecast model results indicate the unusual juxtaposition of two features: 1) strong synoptically driven easterly flow and 2) very cold lower-tropospheric air contributing to a stability profile that favors the enhancement of mountain-wave development by nonlinear effects. Although both of these features do occur with some regularity over Colorado during the cold season, the strength of both features at the same time in this event was unusual. Strong easterly winds over the mountain barrier typically result from a deep cyclonic system, as was the case for the blowdown event. These cyclonic systems, however, are generally not accompanied by an extremely cold boundary layer. Very cold boundary layers are more typically observed with shallow anticyclonic events, which normally generate weaker easterly flow over a portion of the mountain barrier. In this event, a modified arctic air mass was drawn southward into the strong cyclone. The likely explanation for the strong winds is the combination of a deep, very cold boundary layer and strong, cyclonic

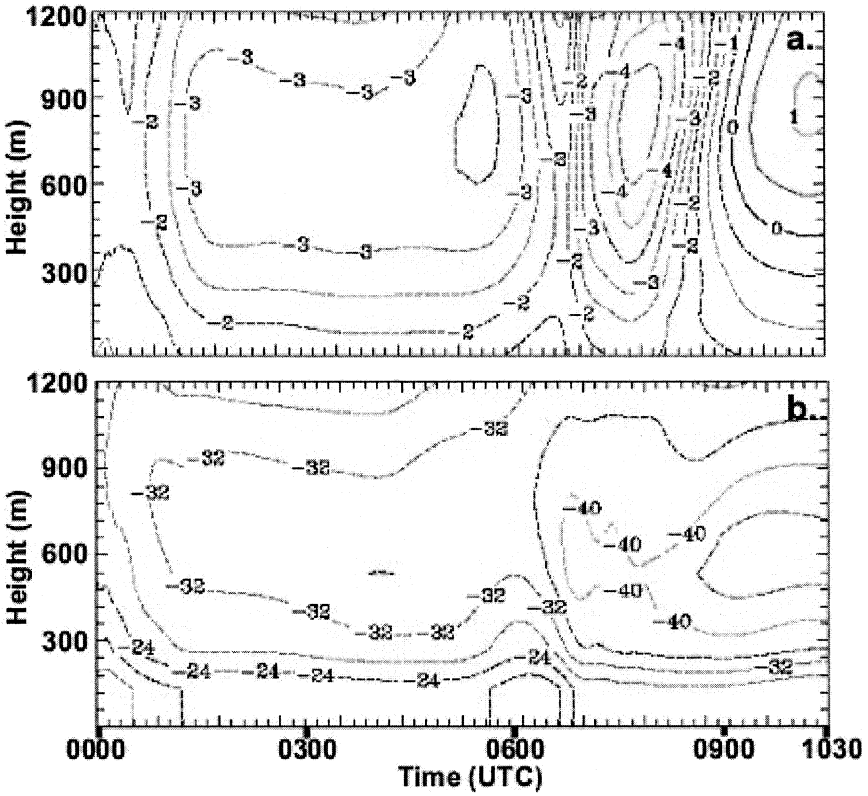

FIG. 13. Time series for simulation II from 0000 UTC (24 h of simulation time) to 1030 UTC 25 Oct 1997 (34.5 h of simulation time) for (a) vertical velocity (m s^{-1}) and (b) the *u* component of the wind (m s^{-1}). Height (AGL) is in meters. Gridpoint location of time series is slightly west of MTE (shown in Fig. 10).

easterly flow over a relatively low mountain barrier, which created the proper conditions to generate a severe downslope windstorm that destroyed many acres of old-growth forest.

The two RAMS simulations have successfully predicted the high winds observed along the Continental Divide of Colorado. These results suggest that the potential exists to capture mesoscale events of this type accurately more than 1 day in advance. These simulations were quasi forecast in nature, because two 48-h Eta forecasts were used to specify the lateral boundary conditions. The results also suggest that the 1.67-km grid spacing simulation provides even greater predictive detail than the coarser-grid simulation for this investigation. Forecast wind speeds were 20% greater in the high-resolution simulation, whereas the coarser-grid simulation was unable to resolve the dual wind maxima found in the higher-resolution run. A simple comparison of the terrain features resolved by the 5-km grid spacing simulation and the 1.67-km grid spacing simulation suggests that adequate depiction of terrain relief is a major factor.

High-resolution, local-area model forecasts provide an important component in formulating conceptual models of highly variable mesoscale events, including the Mount Zirkel Wilderness forest blowdown. This case study demonstrates the capability of predicting these events by using local-area models combined with other operational products. This study has helped to increase the understanding of downslope windstorms along the West Slope of Colorado for the Grand Junction National Weather Service Forecast Office (GJT).

Several high-wind events, albeit weaker and more isolated, have been forecast well subsequent to the 1997 blowdown event, one of which is an event in April of 1999, summarized by Jones et al. (2002). In another event in March of 2000, high winds were forecast several days in advance for Steamboat Springs and the surrounding area by GJT. The resultant storm damaged the ski area with 40 m s^{-1} winds and required a mountain rescue of nearly 300 people who were trapped on the mountain. Increased scrutiny for these kinds of events by the GJT staff indicates that downslope windstorms over the West Slope of the Continental Divide in Colorado may occur more often than initially thought. Therefore, it is important to understand the antecedent conditions responsible for these kind of events in order to alert the public with timely warnings and statements. The inclusion of a high-resolution, local-area model in

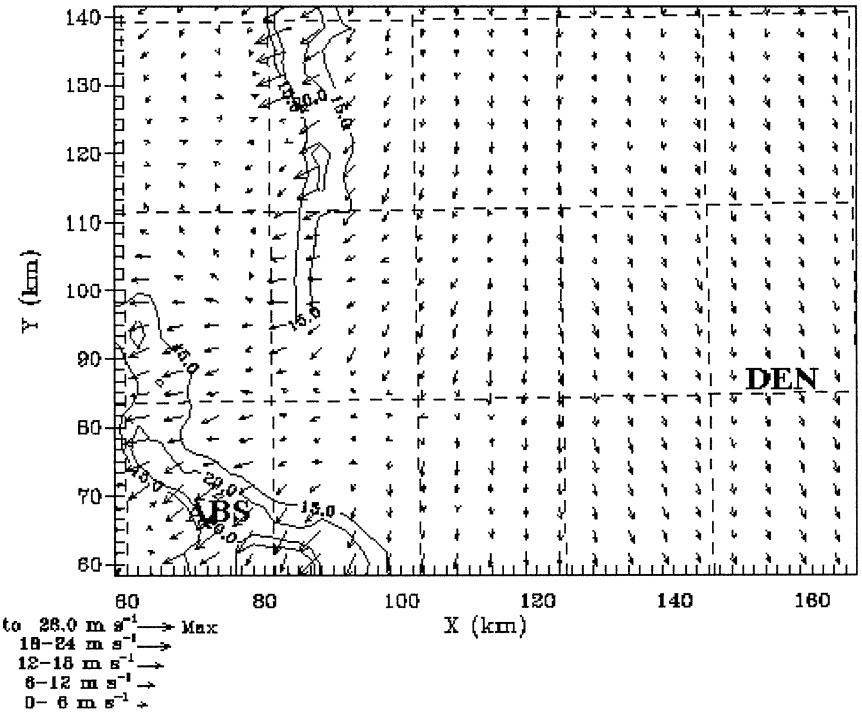

FIG. 14. Plan view of wind speed (m s^{-1}) on grid 3 after 38 h of simulation time, valid at 1400 UTC 25 Oct 1997 for simulation II. Wind speeds are contoured every 5 m s^{-1}, with minimum contour 15 m s^{-1}. Wind arrows are plotted every third grid point, with speed legend at bottom of figure.

the forecasters' set of operational tools would facilitate this process.

Acknowledgments. Drs. William Cotton and Roger Pielke of Colorado State University and Dr. Craig Tremback of Mission Research Corporation are acknowledged for their continued permission to use RAMS for this project. RAMS was developed under the support of the National Science Foundation and the Army Research Office. Drs. Randy Borys and Melanie Wetzel and Mr. Arthur Judson provided observations and accounts in regard to the forest blowdown. Alan Henceroth provided observations from the Arapahoe Basin Ski Area. Lynne Drogosz and Diane Pipher of the USFS provided valuable forest blowdown information. Timothy Alberta, Jeffrey Colton, and Steve Deyo are acknowledged for their graphical work. The authors also thank Kim Runk, Preston Leftwich, and James Pringle for their reviews of the manuscript. Dr. Poulos acknowledges the support of National Science Foundation through Grants ATM-9713073 and ATM-9816160.

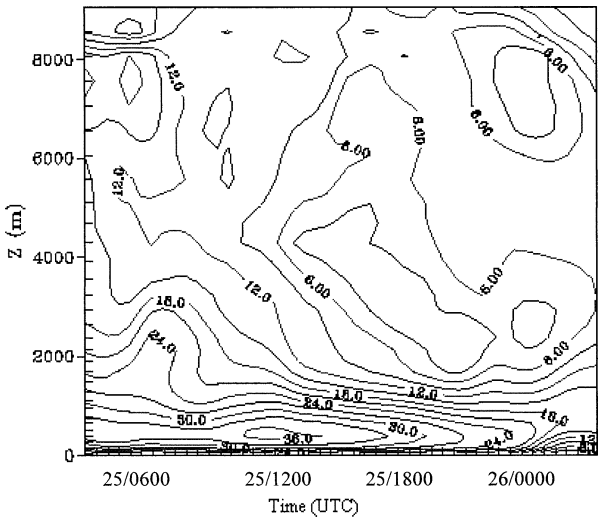

FIG. 15. Time series for simulation II from 0400 UTC 25 Oct 1997 to 0300 UTC 26 Oct 1997 for winds (m s^{-1}). Height (AGL) is in meters. Gridpoint location of time series is located over ABS (Fig. 14).

REFERENCES

Black, T. L., 1994: The new NMC Mesoscale Eta Model: Description and forecast examples. *Wea. Forecasting,* **9,** 265–278.

Borys, R. D., and M. A. Wetzel, 1997: Storm Peak Laboratory: A research, teaching, and service facility for the atmospheric sciences. *Bull. Amer. Meteor. Soc.,* **78,** 2115–2123.

Brown, J. M., A. A. Rockwood, J. F. Weaver, B. D. Jamison, and R. Holmes, 1992: An expert system for the prediction of downslope windstorms. Abstracts, *Fourth Workshop on Operational Meteorology,* Whistler, BC, Canada, Canadian Meteorological and Oceanographic Society/Atmospheric Environment Service.

Carruthers, D. J., and J. C. R. Hunt, 1990: Fluid mechanics of airflow over hills: Turbulence, fluxes and waves in the boundary layer.

Atmospheric Processes over Complex Terrain, Meteor. Monogr., No. 45, Amer. Meteor. Soc., 83–107.

Clark, T. L., and W. R. Peltier, 1977: On the evolution and stability of finite-amplitude mountain waves. *J. Atmos. Sci.,* **34,** 1715–1730.

——, and R. D. Farley, 1984: Severe downslope windstorm calculations in two and three spatial dimensions using anelastic interactive grid nesting. *J. Atmos. Sci.,* **41,** 329–350.

Colle, B. A., and C. F. Mass, 1998a: Windstorms along the western side of the Washington Cascade Mountains. Part I: A high-resolution observational and modeling study of the 12 February 19995 event. *Mon. Wea. Rev.,* **126,** 28–52.

——, and ——, 1998b: Windstorms along the western side of the Washington Cascade Mountains. Part II: Characteristics of past events and three-dimensional idealized simulations. *Mon. Wea. Rev.,* **126,** 53–71.

——, and ——, 2000: High-resolution observations and numerical simulations of easterly gap flow through the Strait of Juan de Fuca on 9–10 December 1995. *Mon. Wea. Rev.,* **128,** 2398–2422.

Cotton, W. R., G. Thompson, and P. W. Mielke Jr., 1994: Real-time mesoscale prediction on workstations. *Bull. Amer. Meteor. Soc.,* **75,** 349–362.

——, J. F. Weaver, and B. A. Beitler, 1995: An unusual summertime downslope wind event in Fort Collins, Colorado, on 3 July, 1993. *Wea. Forecasting,* **10,** 786–797.

Doyle, J. D., and R. B. Smith, 2002: Mountain waves over the Hohe Tauern: Influence of upstream diabatic effects. *Quart. J. Roy. Meteor. Soc.,* **129,** 799–824.

——, and Coauthors, 2000: An intercomparison of model-predicted wave breaking for the 11 January 1972 Boulder windstorm. *Mon. Wea. Rev.,* **128,** 901–914.

Durran, D. R., 1986: Another look at downslope windstorms. Part I: On the development of analogs to supercritical flow in an infinitely deep, continuously stratified fluid. *J. Atmos. Sci.,* **43,** 2527–2543.

——, 1990: Mountain waves and downslope windstorms. *Atmospheric Processes over Complex Terrain, Meteor. Monogr.,* No. 45, Amer. Meteor. Soc., 59–81.

——, 2002: Downslope winds. *Encyclopedia of Atmospheric Sciences,* J. Holton, J. Pyle, and J. Curry, Eds., Elsevier, 644–649.

——, and J. B. Klemp, 1987: Another look at downslope windstorms. Part II: Nonlinear amplification beneath wave-overturning layers. *J. Atmos. Sci.,* **44,** 3402–3412.

Gallus, W. A., Jr., 2000: The impact of step orography on flow in the Eta Model: two contrasting examples. *Wea. Forecasting,* **15,** 630–639.

——, and J. B. Klemp, 2000: Behavior of flow over step orography. *Mon. Wea. Rev.,* **128,** 1153–1164.

Horel, J., T. Potter, L. Dunn, W. J. Steenburgh, M. Eubank, M. Splitt, and D. J. Onton, 2002: Weather support for the 2002 Winter Olympic and Paralympic Games. *Bull. Amer. Meteor. Soc.,* **83,** 227–240.

Jones, C. N., J. D. Colton, R. L. McAnelly, and M. P. Meyers, 2002: A mountain wave event west of the Colorado Park Range. *Natl. Wea. Dig.,* in press.

Klemp, J. B., and D. Lilly, 1975: The dynamics of wave induced downslope winds. *J. Atmos. Sci.,* **32,** 320–330.

Lee, T. J., R. A. Pielke, R. C. Kessler, and J. Weaver, 1989: Influence of cold pools downstream of mountain barriers on downslope winds and flushing. *Mon. Wea. Rev.,* **117,** 2041–2058.

Manobianco, J., G. E. Taylor, and J. W. Zack, 1996: Workstation-based real-time mesoscale modeling designed for weather support to operations at the Kennedy Space Center and Cape Canaveral Air Station. *Bull. Amer. Meteor. Soc.,* **77,** 653–672.

Mass, C. F., and Y. Kuo, 1998: Regional real-time numerical weather prediction current status and future potential. *Bull. Amer. Meteor. Soc.,* **79,** 253–263.

——, D. Ovens, K. Westrick, and B. A. Colle, 2002: Does increasing horizontal resolution produce more skillful forecasts? *Bull. Amer. Meteor. Soc.,* **83,** 407–430.

McQueen, J. T., R. R. Draxler, and G. D. Rolph, 1995: Influences of grid size and terrain resolution on wind field predictions from an operational mesoscale model. *J. Appl. Meteor.,* **34,** 2166–2181.

Peltier, W. R., and T. L. Clark, 1979: The evolution and stability of finite-amplitude mountain waves. Part II: Surface wave drag and severe downslope windstorms. *J. Atmos. Sci.,* **36,** 1498–1529.

Pielke, R. A., and Coauthors, 1992: A comprehensive meteorological modeling system—RAMS. *Meteor. Atmos. Phys.,* **49,** 69–91.

Poulos, G. S., J. E. Bossert, R. A. Pielke, and T. B. McKee, 2000: The interaction of katabatic flow and mountain waves. Part I: Observations and idealized simulations. *J. Atmos. Sci.,* **57,** 1919–1936.

——, D. A. Wesley, J. S. Snook, and M. P. Meyers, 2002: A Rocky Mountain storm. Part I: The blizzard—Kinematic evolution and the potential for high-resolution numerical forecasting of snowfall. *Wea. Forecasting,* **17,** 955–970.

Schultz, P., 1995: An explicit cloud physics parameterization for operational numerical prediction. *Mon. Wea. Rev.,* **123,** 3331–3343.

Smith, R. B., 1985: On severe downslope winds. *J. Atmos. Sci.,* **42,** 2597–2603.

——, 1987: Aerial observations of the Yugoslavian bora. *J. Atmos. Sci.,* **44,** 269–297.

Snook, J. S., and R. A. Pielke, 1995: Diagnosing a Colorado heavy snow event with a nonhydrostatic mesoscale numerical model structured for operational use. *Wea. Forecasting,* **10,** 261–285.

——, J. M. Cram, and J. M. Schmidt, 1995: LAPS/RAMS: A nonhydrostatic modeling system configured for operational use. *Tellus,* **47A,** 864–875.

——, P. A. Stamus, J. Edwards, Z. Christidis, and J. A. McGinley, 1998: Local-domain mesoscale analysis and forecast model support for the 1996 Centennial Olympic Games. *Wea. Forecasting,* **13,** 138–150.

Svejkovsky, J., 1985: Santa Ana airflow observed from wildfire smoke patterns in imagery. *Mon. Wea. Rev.,* **113,** 902–906.

Walko, R. L., W. R. Cotton, M. P. Meyers, and J. L. Harrington, 1995: New RAMS cloud microphysics parameterization. Part I: The single-moment scheme. *Atmos. Res.,* **38,** 29–62.